

Verification Analysis for a High Pressure Sequence of TLOFW in APR1400 using CINEMA Computer Code

Rae-Joon Park ^{a*}, Dong Gun Son ^a, Jaehoon Jung ^a

^aKorea Atomic Energy Research Institute, 1045 Daedeok-daero, Yuseong-Gu, Daejeon, Korea

*Corresponding author: rjpark@kaeri.re.kr

***Keywords** : severe accident, CINEMA, verification analysis, TLOFW, APR1400

1. Introduction

As an integrated severe accident computer code development in Korea, CINEMA (Code for INtegrated severe accidEnt Management Analysis) has been developed for a stand-alone severe accident analysis [1]. The basic goal of this code development is to design a severe accident analysis code package by exploiting the existing domestic DBA (Design Basis Analysis) code system for the severe accident analysis. The CINEMA computer code are composed of CSPACE [2], SACAP (Severe Accident Containment Analysis Package) [3], and SIRIUS (SIMulation of Radioactive nuclide Interaction Under Severe accident) [4], which are capable of core melt progression with thermal hydraulic analysis of the RCS (Reactor Coolant System), severe accident analysis of the containment, and fission product analysis, respectively, as shown in Fig. 1.

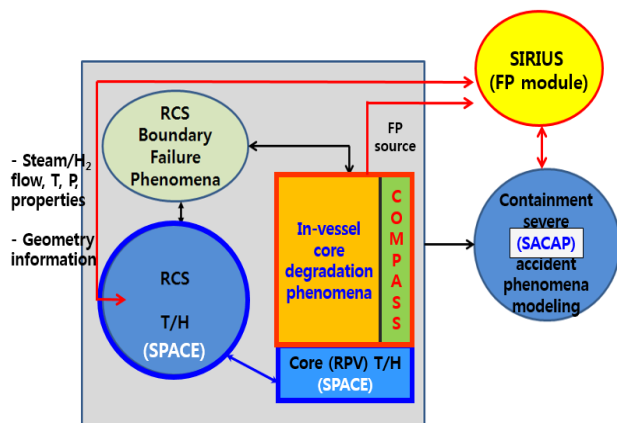


Fig.1 CINEMA code structure.

For the purpose of CINEMA verification for a real power plant, a high RCS (Reactor Coolant System) pressure sequence of TLOFW (Total Loss Of Feed Water) for the APR1400 [8] has been analyzed in this study. This analysis has been performed to estimate the efficiency of the CINEMA computer code and the predictive qualities of its models from an initiating event to a reactor vessel failure.

2. CINEMA Input Model for APR1400

The input model for the CSPACE calculation of the CINEMA for the APR1400 was a combination of the SPACE and COMPASS input models. Heat structures for the fuel rods and the lower part of the reactor vessel in the SPACE input model were replaced by the COMPASS input models. In the SPACE model, the reactor core was simulated as 3 channels to evaluate the thermal-hydraulic behavior in detail, and each channel was composed of 5 axial volumes, as shown in Fig. 2. A surge line and a pressurizer were attached to one of the hot legs in the primary coolant loop. In the COMPASS input model of this study, the component numbers for the fuel and the control rods were 3 and 3. The axial node number of the fuel and control rods was 5 each, and the radial node numbers for the fuel and the control rods were 3 and 3, respectively.

A steady state calculation was performed in order to verify the input nodalization. The steady state results of the CINRMA calculation for a selected set of parameter were in very good agreement with the integral reactor operating conditions. The steady state results obtained from the simulation were used as initial conditions for the transient calculation.

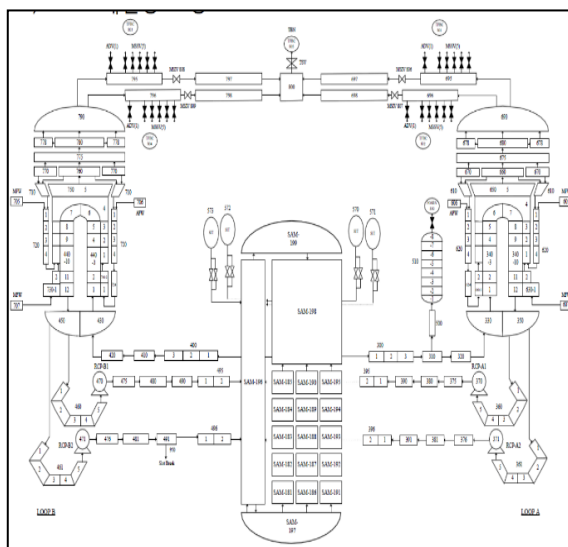


Fig. 2. CINEMA input model for the nuclear steam supply system in APR1400.

3. Results and Discussion

The TLOFW transient is initiated when the main and auxiliary feedwater are lost, and is assumed to occur at 0 sec. The accident sequence scenarios for the TLOFW transient follow the case which has the highest probability of occurrence based on the results of level 1 PSA analysis [8]. Since the main and auxiliary feedwater are not supplied to both steam generators following the transient at 0 sec., the steam generator secondary side water level decreases due to the steam generation by boiling and finally the steam generators cannot act as effective heat sinks any more when the steam generator secondary sides dry up. The reactor and the RCP are tripped due to the low steam generator level and coolant sub-cooling margin, respectively. Since the decay heat is eliminated by the steam generators due to the decreased steam generator secondary side's water level, the pressure and temperature of the RCS increase. The SRVs (Safety Relief Valves) of the steam generator regulated the pressure of the secondary side. The RCS pressure increases up to 17.3 MPa, which is the opening pressure of the pressurizer POSRVs (Power Operated Safety Relief Valves). Following this time, the RCS pressure fluctuates between the opening (17.3 MPa) and closing pressure (15.6 MPa) of the pressurizer POSRV.

Boiling starts to occur in the reactor core, which causes core uncovering at the top of the fuel rods. Fuel rod cladding temperature increases since heat transfer from the fuel rod to the surrounding coolant decreases following the initiation of core uncovering. As the fuel rod temperature increases, the internal pressure of the fuel rod increases since fission products in the fuel rod are released to the gap between the fuel rod and the cladding. When the cladding temperature reaches 1,173K, the cladding fails at 9,018 sec in the TLOFW transient, which results in the gap release of the fission products.

Oxidation of the fuel cladding began when the cladding surface temperature reached 1,000 K and produced oxidation heat. When the fuel rod temperature reaches 1700 K, the fuel rod cladding oxidation occurs vigorously and the cladding temperature increases rapidly due to oxidation heat generation in the core. ZrO₂ is ruptured and relocated to the lower part of the core when the fuel rod cladding temperature reaches 2,500 K. At this time the dissolved fuel rod is also relocated to the lower core and formed a cohesive debris bed. The molten material slumps to the lower plenum of the reactor vessel at 40,800 sec. Finally, the reactor lower head vessel failure occurs at 41,121 sec in the TLOFW transient.

Fig. 3 show the pressurizer pressure during the TLOFW transient. When the TLOFW transient occurs at 0 sec, the main feedwater is not supplied to the steam generator and the MSIV is closed. For this reason, the steam generator secondary side pressure increases up to the setting pressure (8.75 MPa) of the SRV. The RCS pressure increases slightly due to the reduced heat transfer through the steam generator U-tubes, and then decreases due to the reduced core decay power. The RCS

pressure increases up to the setting pressure of the pressurizer POSRV (17.3 MPa), and then the RCS inventory is lost through the opened POSRV. When the RCS pressure decreases to the closing setting pressure of the POSRV (15.6 MPa), the POSRV closes and the pressure builds up again. The RCS pressure fluctuates between the opening and closing setting pressure of the pressurizer POSRV. The pressurizer pressure rapidly decreases to the SITs set point in the RCS depressurization using the POSRV at 5,180 sec, which is 1,800 sec after the SAMG entering condition reaches. When the injected water entered the core from the SITs, it boiled, raising the pressurizer pressure. The increased pressure terminated the coolant injection by SITs actuation, and the pressure decreased again. When the pressure decreased low enough again, more coolant was injected. This cycling of the SITs actuation slowed the depressurization. When the molten core material relocated to the lower plenum, the pressurizer pressure increased slowly, because of coolant boiling in the lower plenum of the reactor vessel

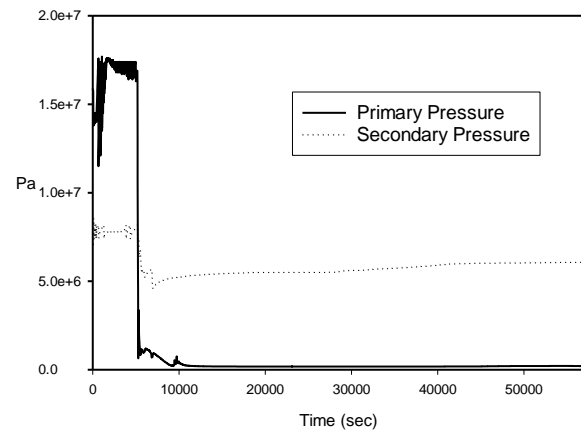


Fig. 3 CINEMA results on the pressurizer pressure in the TLOFW of APR1400.

Figs. 4 and 5 shows the fuel cladding and fuel temperatures in the TLOFW, respectively. The fuel cladding and fuel temperatures are slightly higher than the surrounding coolant temperature until the coolant in the core volume corresponding to each fuel rod is vaporized. Fuel surface temperature at the top of the fuel rods rises when a core uncovering occurs at the top of the core. When the fuel cladding temperature rises up to 1,000 K, a fuel cladding oxidation begins. Following this time, the fuel temperature rises abruptly due to a core oxidation heat generation. The fuel temperature rises abruptly due to a vigorous core oxidation heat generation when the fuel cladding temperature reaches 1,700 K. This temperature rise stops when the fuel cladding temperature reaches 2,500 K because the ZrO₂ is ruptured by a melting and relocated to the lower core at this temperature. When the fuel temperature reaches

2,500 K, the UO_2 is melted and relocated to the lower part of the core, as shown in Figs 6 and 7.

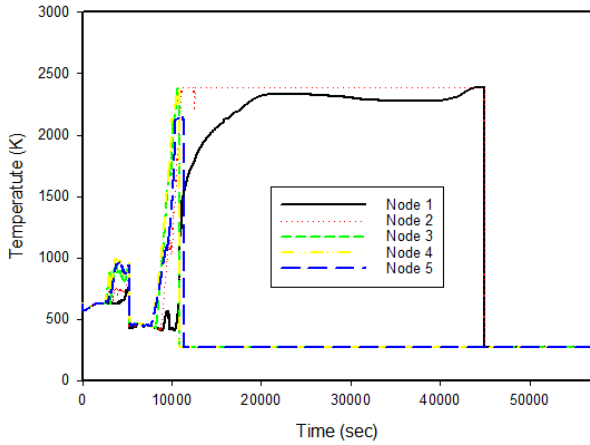


Fig. 4 CINEMA results on fuel cladding temperature in the TLOFW of APR1400.

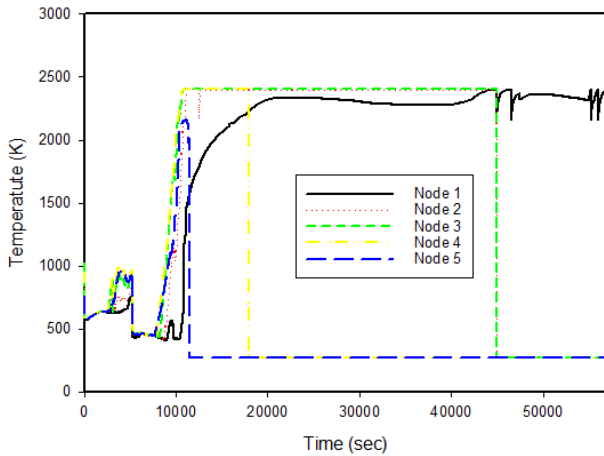


Fig. 5 CINEMA results on fuel temperature in the TLOFW of APR1400.

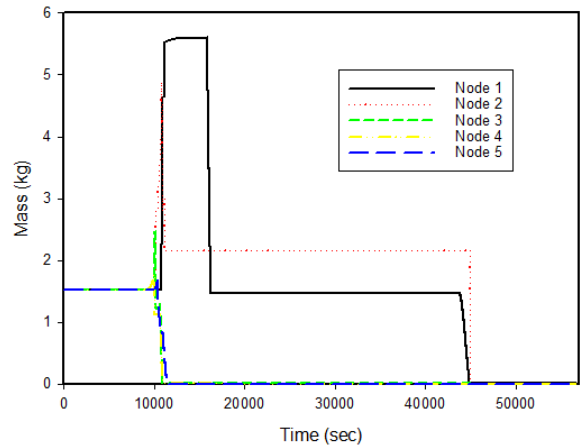


Fig. 6 CINEMA results on fuel cladding mass in the TLOFW of APR1400.

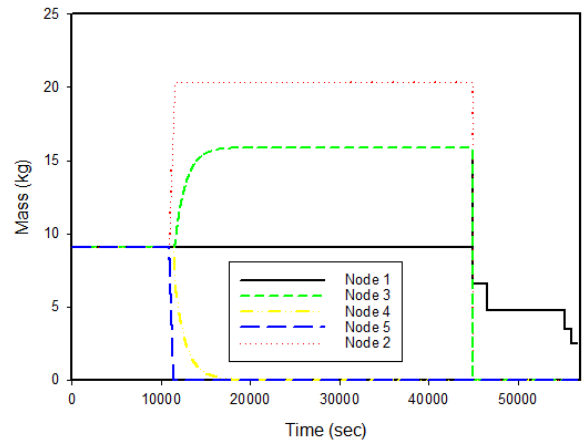


Fig. 7 CINEMA results on fuel mass in the TLOFW of APR1400.

Total hydrogen generation mass in the core is shown in Fig. 8. Hydrogen from oxidation of the fuel cladding is generated in the core when the fuel cladding temperature rises up to 1,000 K. When the fuel cladding temperature reaches 1,700 K, hydrogen generation rate has the peak value due to the vigorous oxidation at this temperature. The total hydrogen generation mass is 353.6 kg, which is approximately 35 % of the fuel rod cladding in TLOFW sequence of the APR1400.

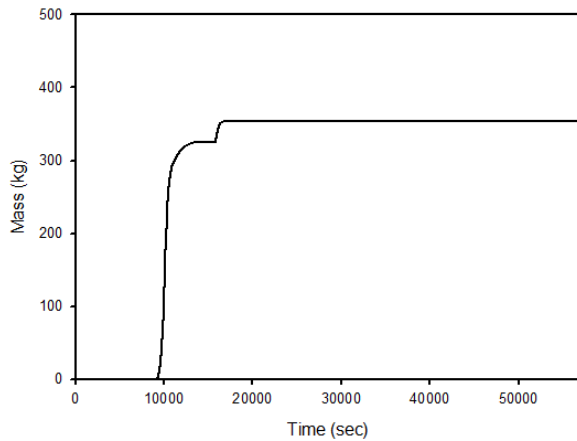


Fig. 8 CINEMA results on the integrated hydrogen generation mass in the TLOFW of APR1400.

Fig. 9 shows the corium mass in the lower plenum of the reactor vessel in the TLOFW transient. The melted core material is initially relocated to the lower plenum at 40,800 sec. Fig. 10 shows the vessel structure temperature in the TLOFW transient. When the large melt material in the lower part of the core relocated to the lower plenum of the reactor vessel, the vessel structure temperature is rapidly increased. Finally, the reactor vessel failed at 41,121 sec.

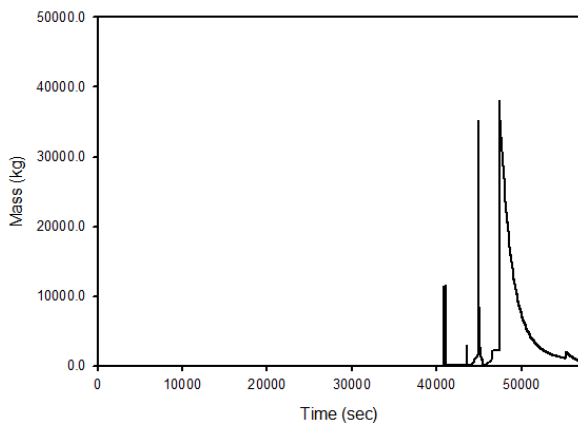


Fig. 9 CINEMA results on corium mass in the lower plenum in the TLOFW of APR1400.

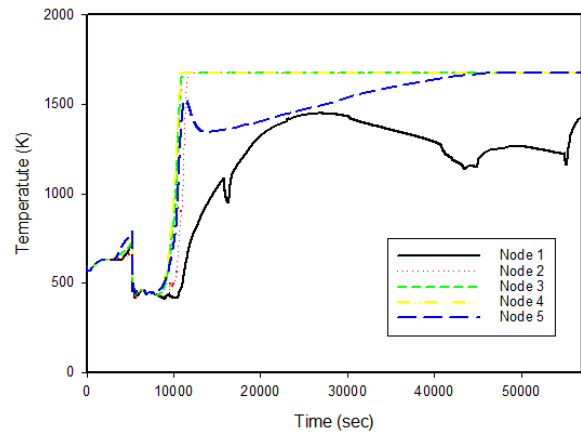


Fig. 10 CINEMA results on the lower head vessel temperature in the TLOFW of APR1400.

4. Conclusion

For the purpose of CINEMA verification for a real power plant, a high RCS pressure sequence of the TLOFW for the APR1400 has been analyzed. This analysis has been performed to estimate the efficiency of the CINEMA computer code and the predictive qualities of its models from an initiating event to a reactor vessel failure. The main results of CINEMA shows the reasonable values in the physical point. More detailed analysis is necessary to validate the CINEMA computer code in the containment performance and fission product behavior for the APR1400.

ACKNOWLEDGMENTS

This work was supported by Nuclear Research & Development Program of the Korea Science and Engineering Foundation (KOSEF) grant funded by the Korean government (MEST). (M20702040004-08M0204-00410)

REFERENCES

- [1] KHNP, KAERI, FNC, KEPCO E&C, "CINEMA User Manual," S11NJ16-2-E-TR-7.4, Rev. 0, 2018.
- [2] J.H. Song, D.G. Son, J.H. Bae, S.W. Bae, K.S. Ha, Chung, B.D., Choi, Y.J. "CSPACE for a Simulation of Core Damage Progression during Severe Accidents," Nuclear Engineering and Technology, 53, 2021.
- [3] FNC, "SACAP User Manual," S11NJ16-2-E-TR-7.4, Rev. 0., 2017.
- [4] K.S. Ha, S.I. Kim, H.S. Kang, D.H. Kim, "SIRIUS: a Code on Fission Product Behavior under Severe Accident," Transactions of the Korean Nuclear Society Spring Meeting, Jeju, Korea, 2017.
- [5] S.J. Ha, "Development of the SPACE Code for Nuclear Power Plants," Nuclear Engineering and Technology, 43, 2011.
- [6] KHNP, KEPCO E&C, KAERI, "SPACE User Manual," S06NX08-K-1-TR-36, Rev. 0, 2017.
- [7] KHNP, KEPCO E&C, KAERI, "SPACE Theoretical Manual," S06NX08-K-1-TR-36, Rev. 0, 2017.
- [8] KEPCO, "Standard Safety Analysis Report", Korea Electric Power Corporation, 1999.